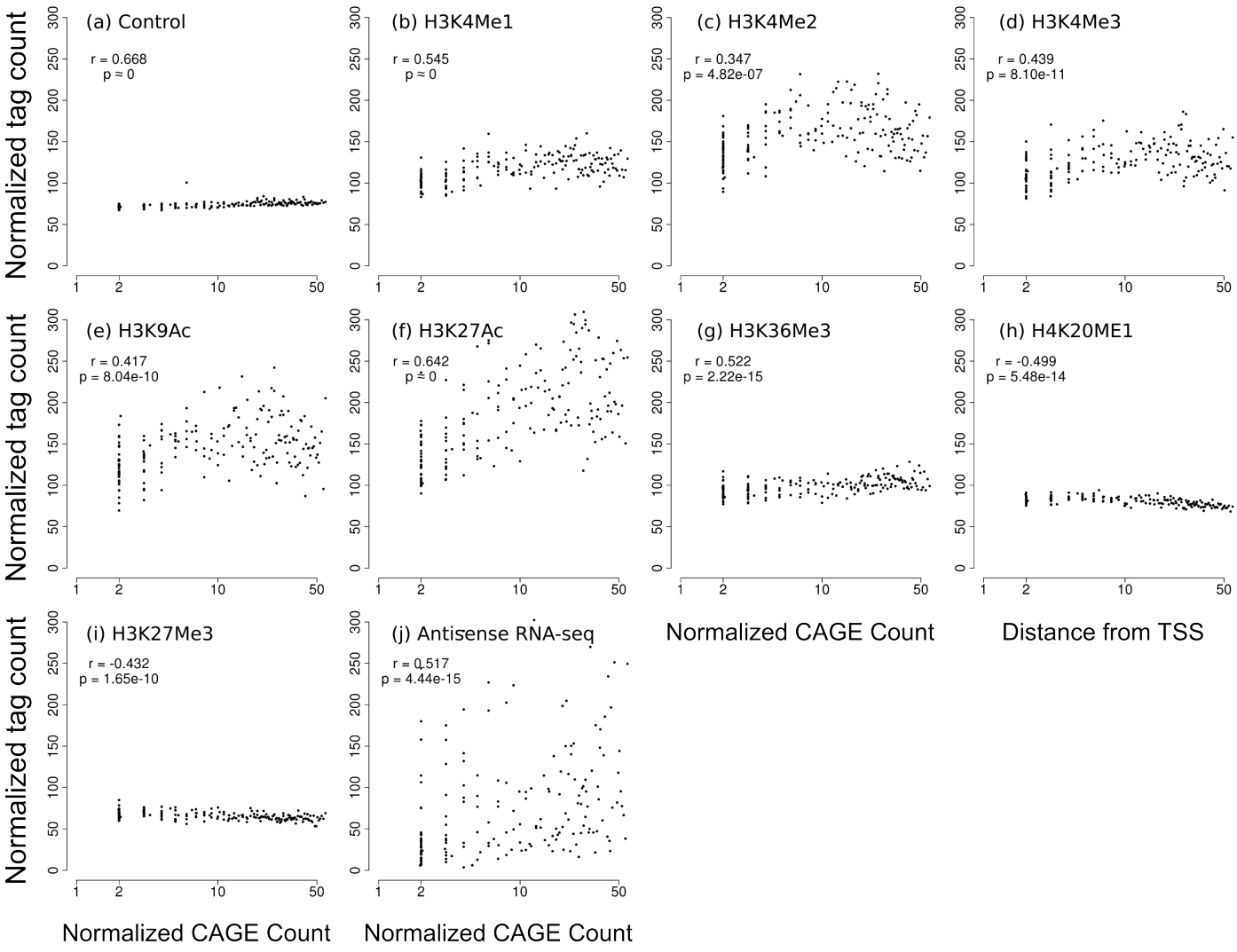

Supplementary Figure S16. Correlation between cis-NAT promoter activity and local chromatin environment in GM12878. Cis-NAT promoters in the GM12878 cell type were identified using CAGE data from non-polyadenylated cytosol isolates. Cis-NAT promoters were divided into 200 bins based on activity, as measured by CAGE tags counts, and the normalized average numbers of ChIP-seq reads for histone modifications +/- 5kb of the cis-NAT TSS were calculated. Spearman rank correlations were used to determine the relationship between cis-NAT promoter activity and local histone modifications.

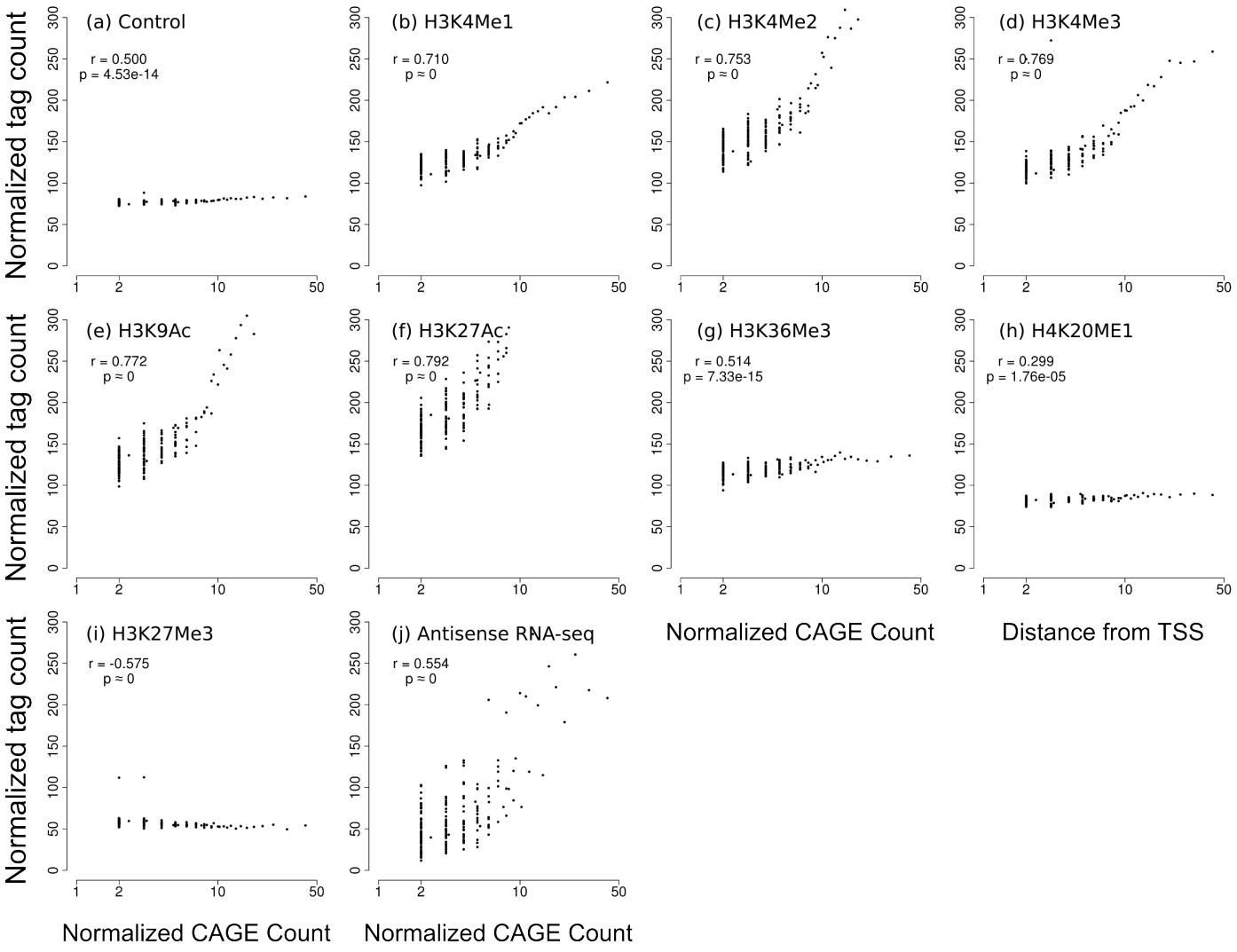

Supplementary Figure S17. Correlation between cis-NAT promoter activity and local chromatin environment in GM12878. Cis-NAT promoters in the GM12878 cell type were identified using CAGE data from total nucleolus isolates. Cis-NAT promoters were divided into 200 bins based on activity, as measured by CAGE tags counts, and the normalized average numbers of ChIP-seq reads for histone modifications +/- 5kb of the cis-NAT TSS were calculated. Spearman rank correlations were used to determine the relationship between cis- NAT promoter activity and local histone modifications.

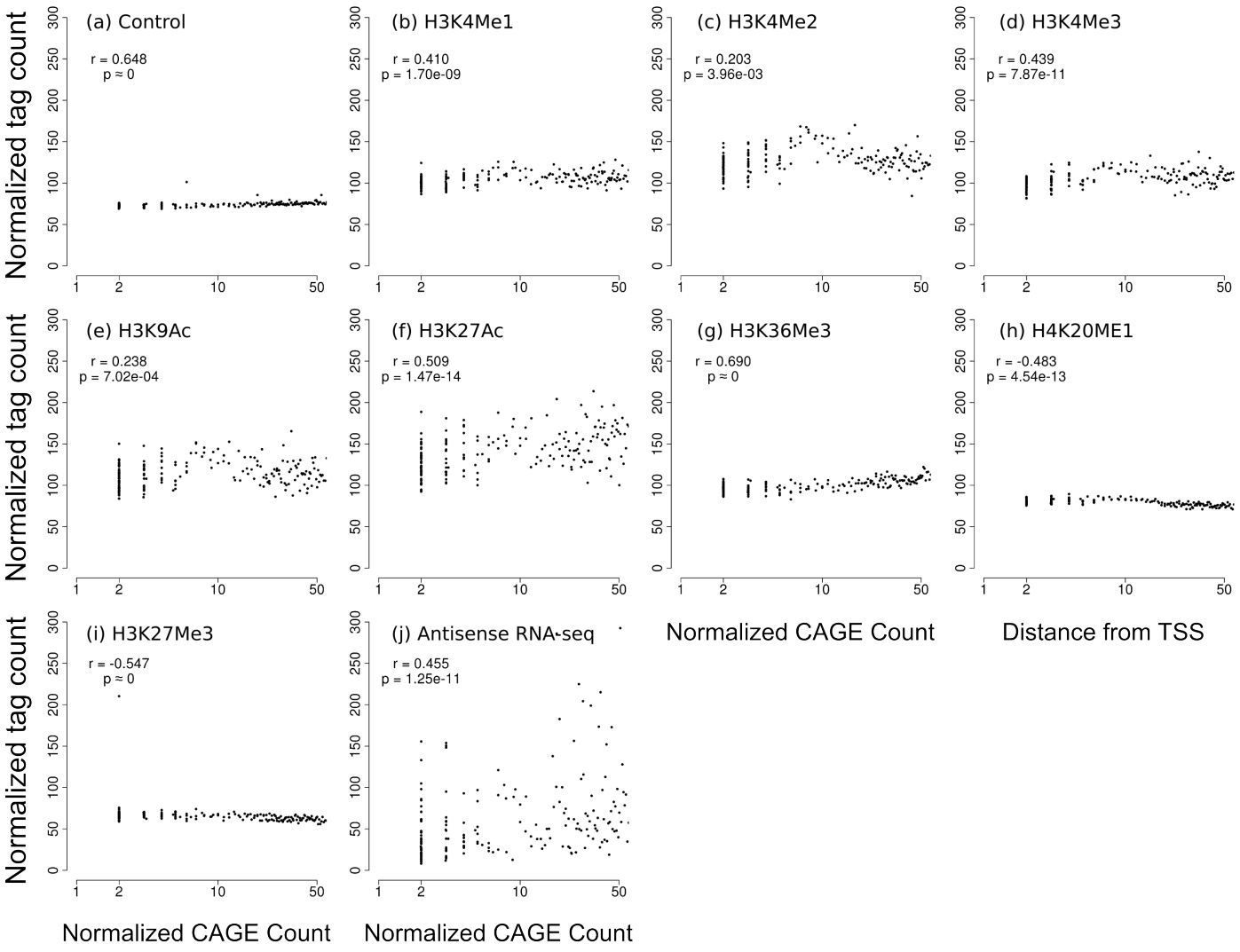

Supplementary Figure S18. Correlation between cis-NAT promoter activity and local chromatin environment in GM12878. Cis-NAT promoters in the GM12878 cell type were identified using CAGE data from non-polyadenylated nucleus isolates. Cis-NAT promoters were divided into 200 bins based on activity, as measured by CAGE tags counts, and the normalized average numbers of ChIP-seq reads for histone modifications +/- 5kb of the cis-NAT TSS were calculated. Spearman rank correlations were used to determine the relationship between cis-NAT promoter activity and local histone modifications.

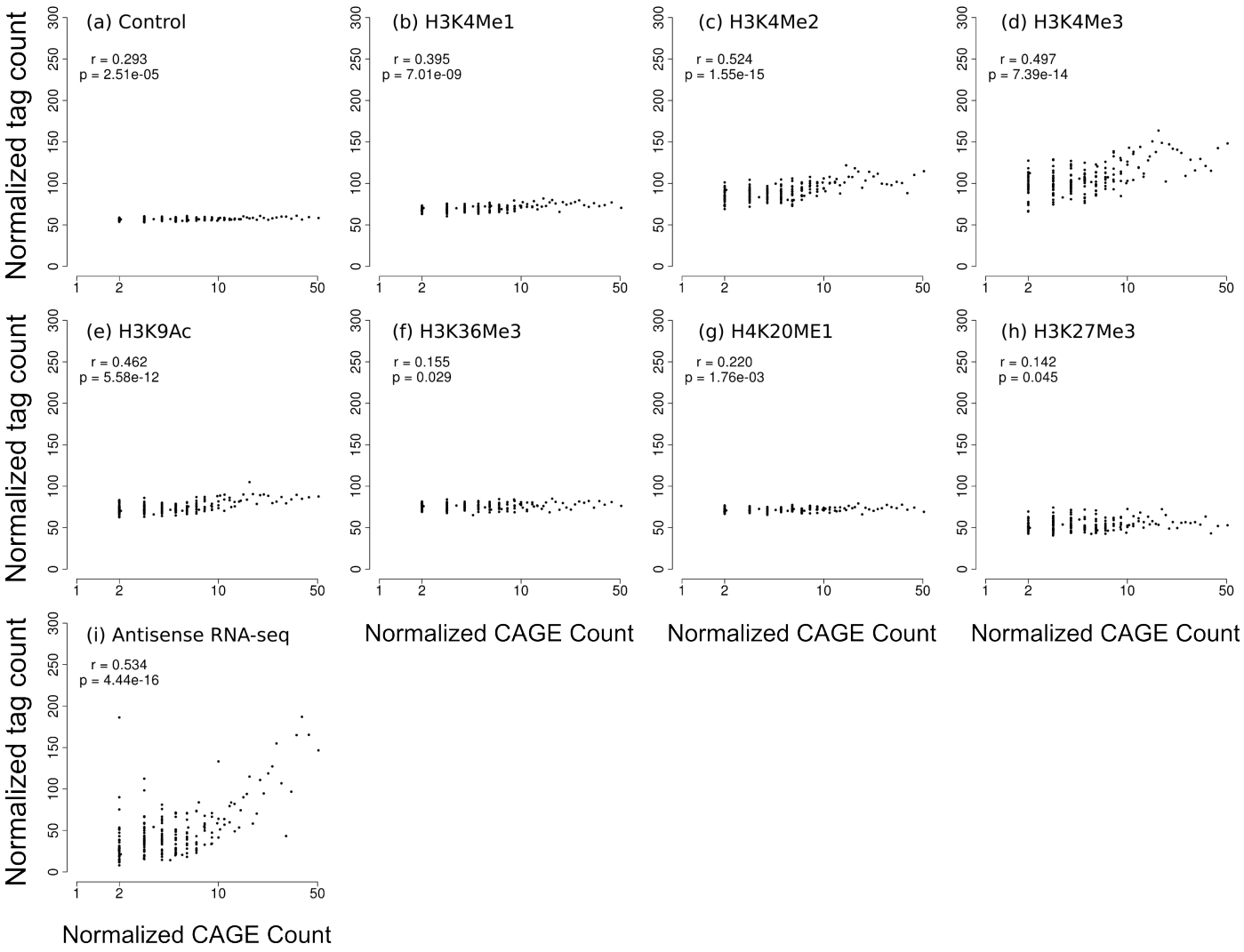

Supplementary Figure S19. Correlation between cis-NAT promoter activity and local chromatin environment in H1HESC. Cis-NAT promoters in the H1HESC cell type were identified using CAGE data from non-polyadenylated whole-cell isolates. Cis-NAT promoters were divided into 200 bins based on activity, as measured by CAGE tags counts, and the normalized average numbers of ChIP-seq reads for histone modifications +/- 5kb of the cis-NAT TSS were calculated. Spearman rank correlations were used to determine the relationship between cis-NAT promoter activity and local histone modifications**.**

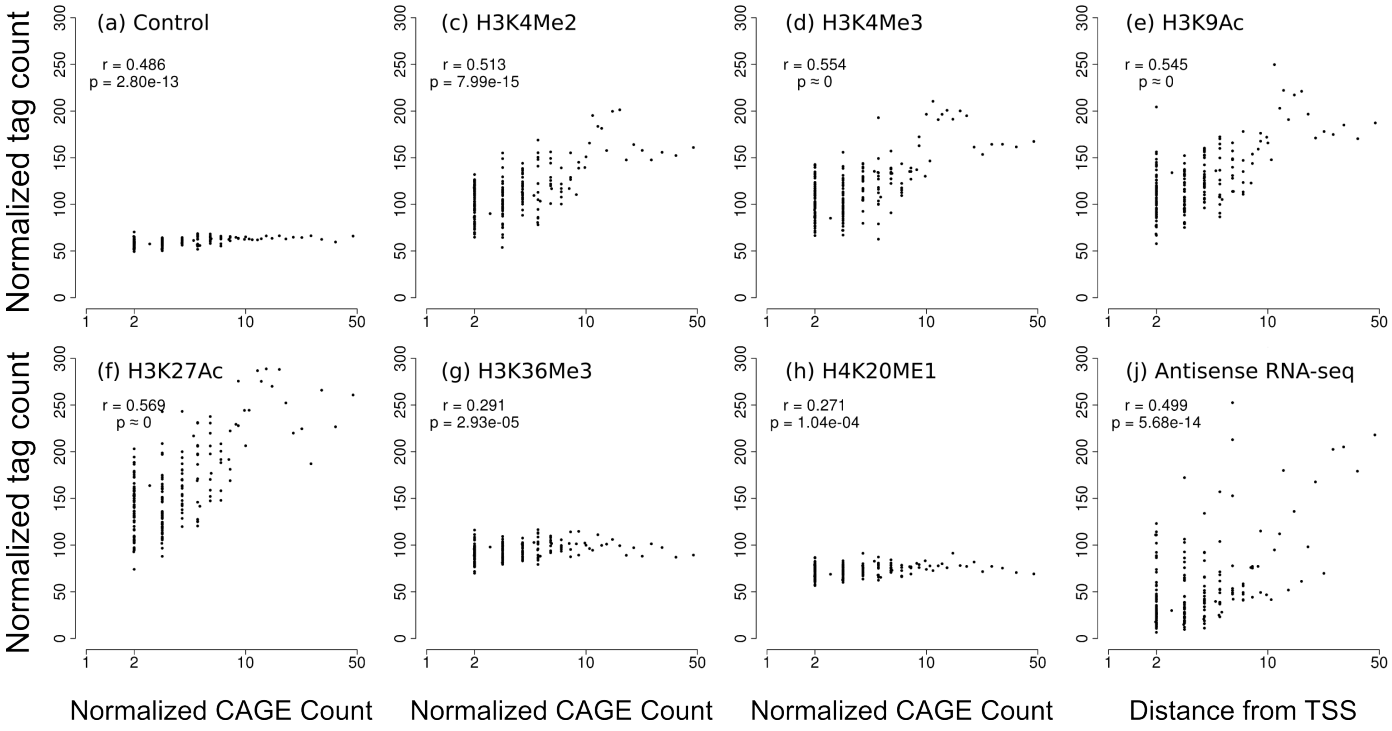

Supplementary Figure S20. Correlation between cis-NAT promoter activity and local chromatin environment in HepG2. Cis-NAT promoters in the HepG2 cell type were identified using CAGE data from non-polyadenylated cytosol isolates. Cis-NAT promoters were divided into 200 bins based on activity, as measured by CAGE tags counts, and the normalized average numbers of ChIP-seq reads for histone modifications +/- 5kb of the cis-NAT TSS were calculated. Spearman rank correlations were used to determine the relationship between cis- NAT promoter activity and local histone modifications.

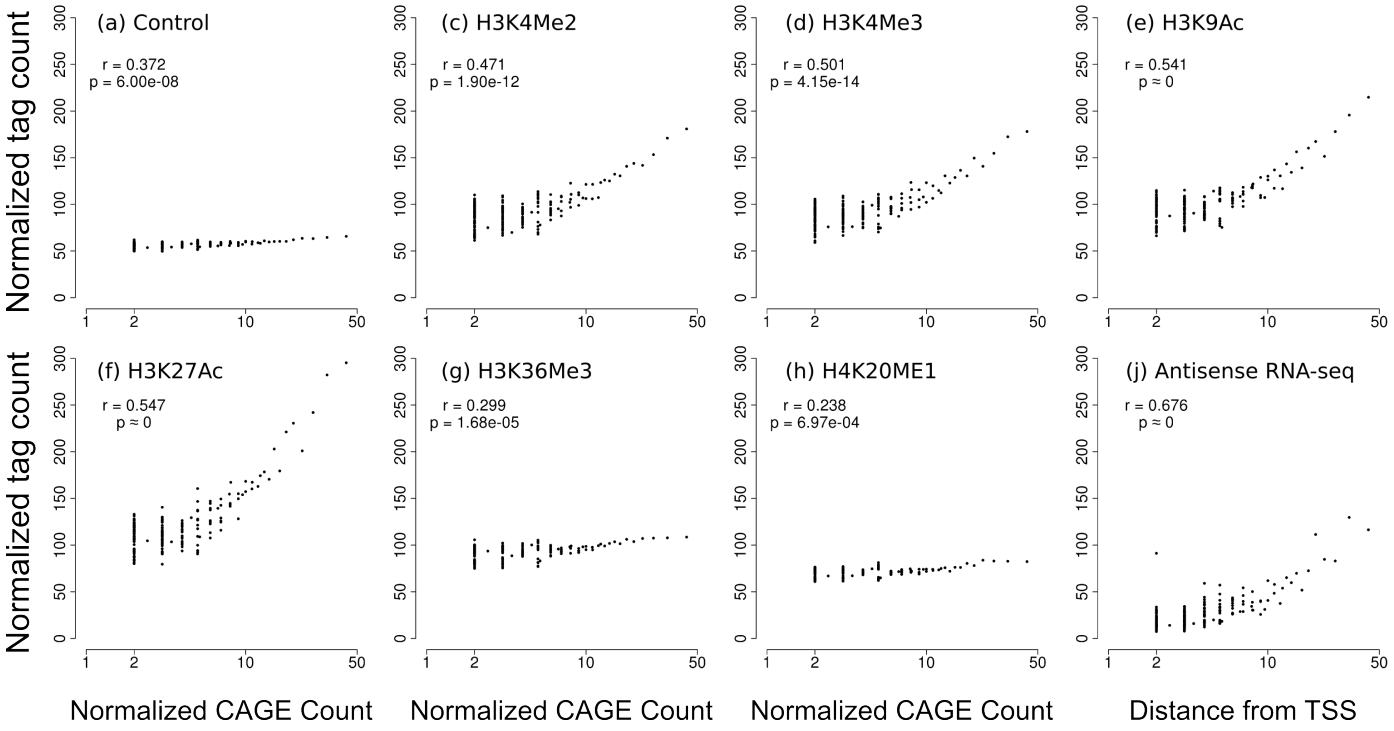

Supplementary Figure S21. Correlation between cis-NAT promoter activity and local chromatin environment in HepG2. Cis-NAT promoters in the HepG2 cell type were identified using CAGE data from total nucleolus isolates. Cis-NAT promoters were divided into 200 bins based on activity, as measured by CAGE tags counts, and the normalized average numbers of ChIP-seq reads for histone modifications +/- 5kb of the cis-NAT TSS were calculated. Spearman rank correlations were used to determine the relationship between cis- NAT promoter activity and local histone modifications.

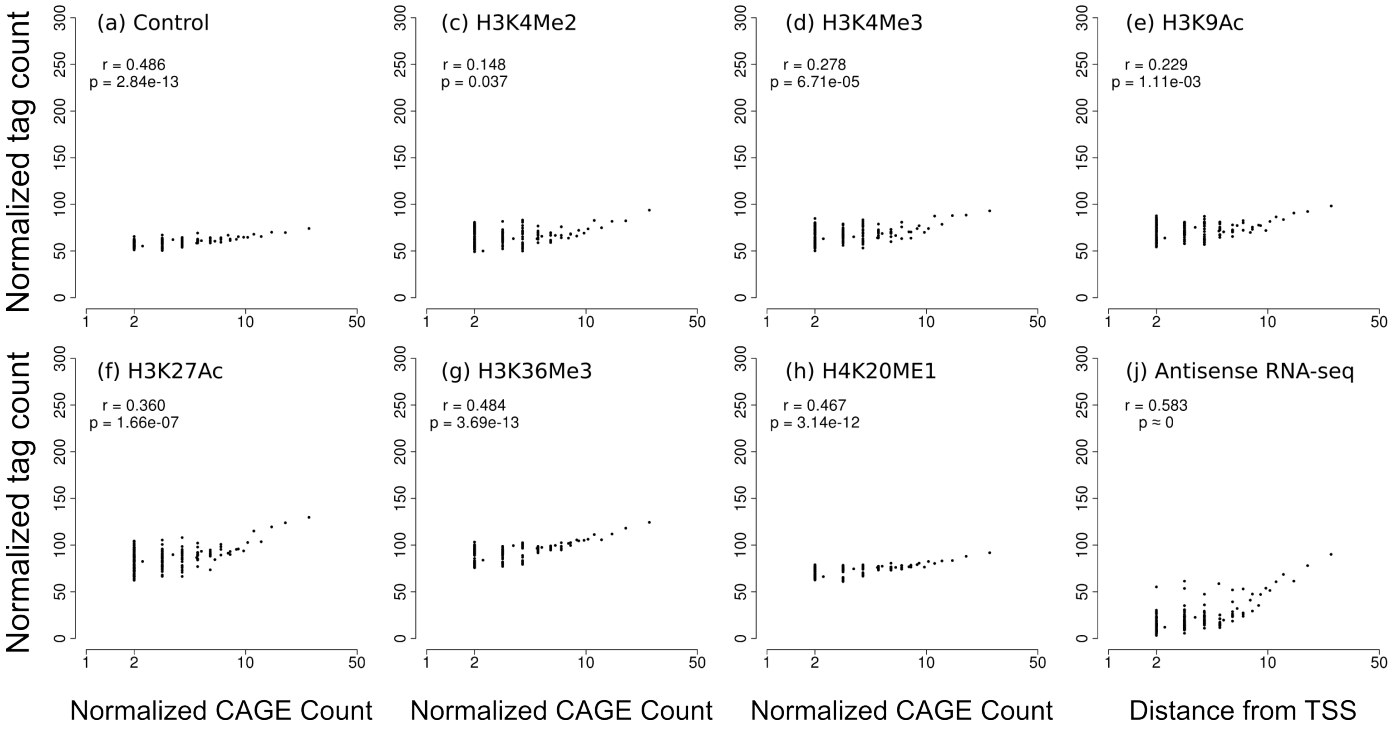

Supplementary Figure S22. Correlation between cis-NAT promoter activity and local chromatin environment in HepG2. Cis-NAT promoters in the HepG2 cell type were identified using CAGE data from non-polyadenylated nucleus isolates. Cis-NAT promoters were divided into 200 bins based on activity, as measured by CAGE tags counts, and the normalized average numbers of ChIP-seq reads for histone modifications +/- 5kb of the cis-NAT TSS were calculated. Spearman rank correlations were used to determine the relationship between cis- NAT promoter activity and local histone modifications.

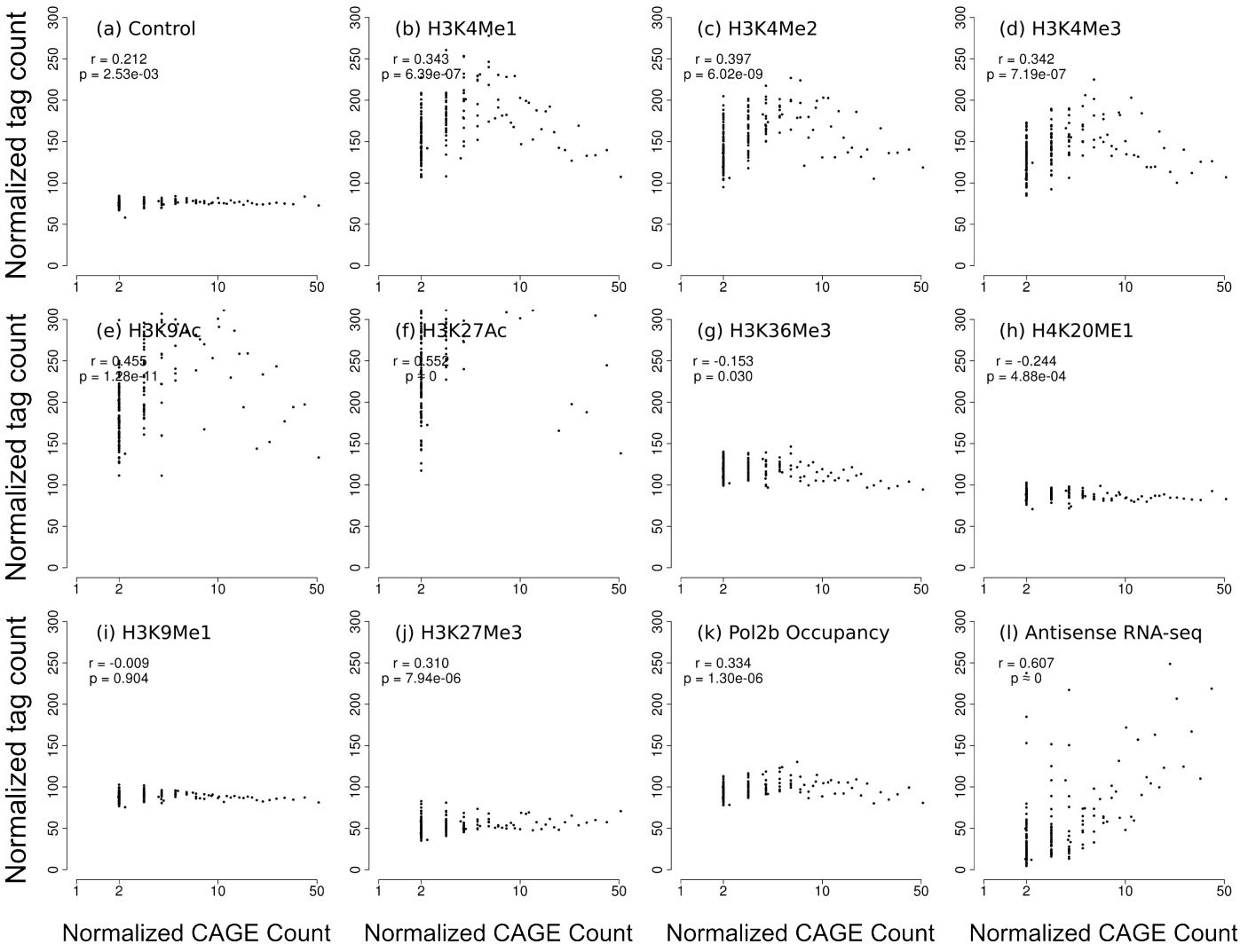

Supplementary Figure S23. Correlation between cis-NAT promoter activity and local chromatin environment in HUVEC. Cis-NAT promoters in the HUVEC cell type were identified using CAGE data from non-polyadenylated cytosol isolates. Cis-NAT promoters were divided into 200 bins based on activity, as measured by CAGE tags counts, and the normalized average numbers of ChIP-seq reads for histone modifications and RNA Pol II binding +/- 5kb of the cis-NAT TSS were calculated. Spearman rank correlations were used to determine the relationship between cis-NAT promoter activity and local histone modifications or RNA Pol II occupancy.

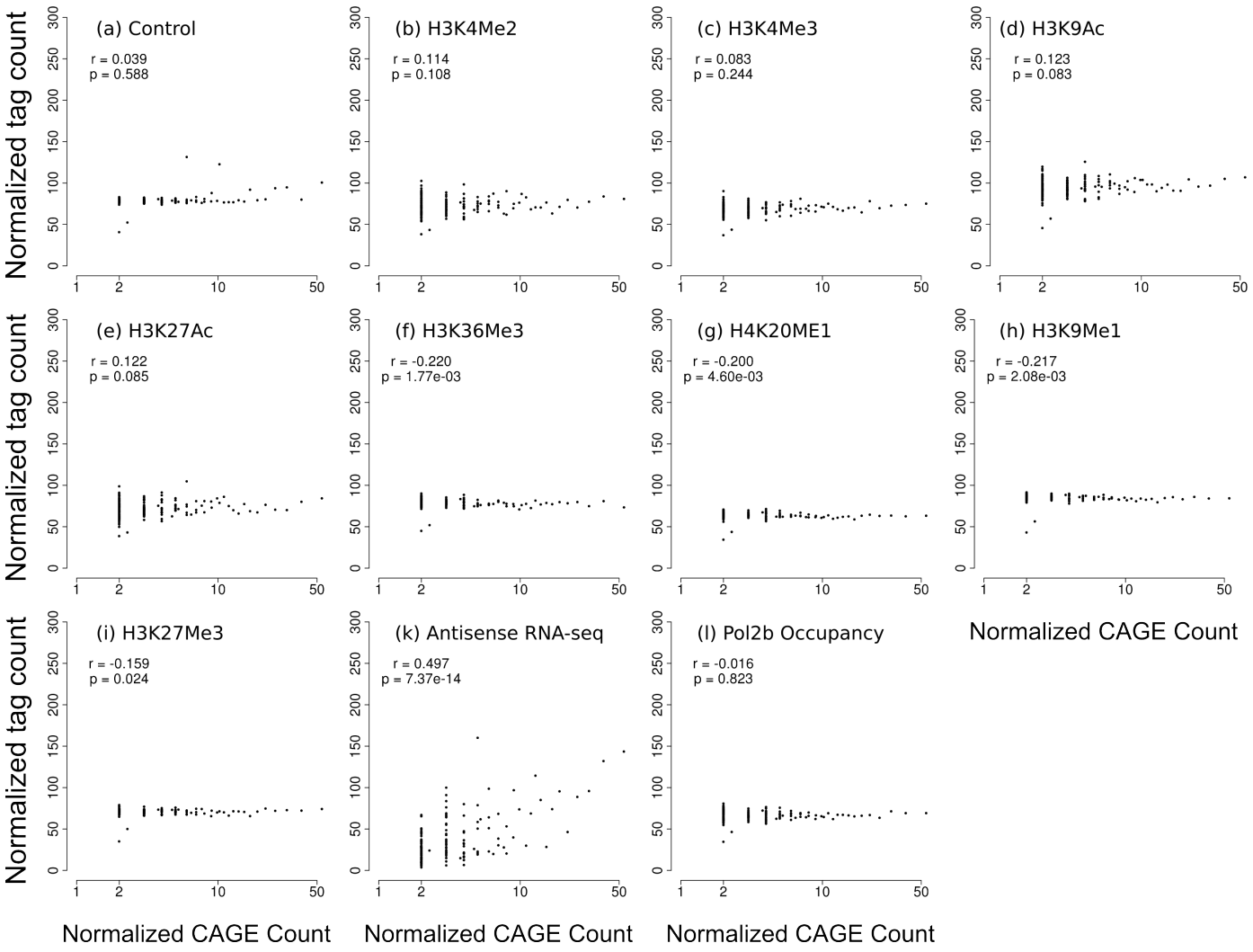

Supplementary Figure S24. Correlation between cis-NAT promoter activity and local chromatin environment in K562. Cis-NAT promoters in the K562 cell type were identified using CAGE data from non-polyadenylated cytosol isolates. Cis-NAT promoters were divided into 200 bins based on activity, as measured by CAGE tags counts, and the normalized average numbers of ChIP-seq reads for histone modifications and RNA Pol II binding +/- 5kb of the cis-NAT TSS were calculated. Spearman rank correlations were used to determine the relationship between cis-NAT promoter activity and local histone modifications or RNA Pol II occupancy.

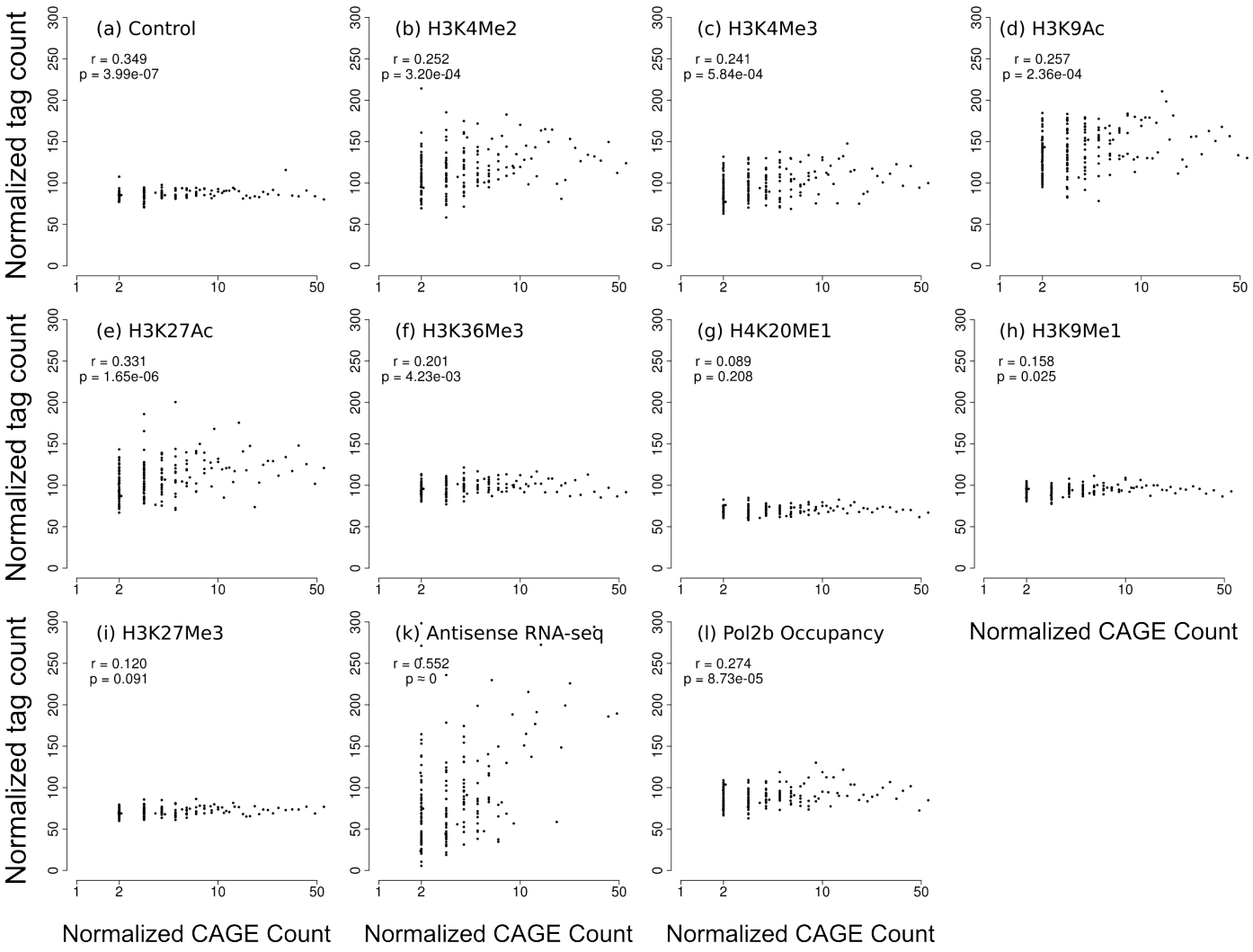

Supplementary Figure S25. Correlation between cis-NAT promoter activity and local chromatin environment in K562. Cis-NAT promoters in the K562 cell type were identified using CAGE data from polyadenylated cytosol isolates. Cis-NAT promoters were divided into 200 bins based on activity, as measured by CAGE tags counts, and the normalized average numbers of ChIP-seq reads for histone modifications and RNA Pol II binding +/- 5kb of the cis-NAT TSS were calculated. Spearman rank correlations were used to determine the relationship between cis-NAT promoter activity and local histone modifications or RNA Pol II occupancy.

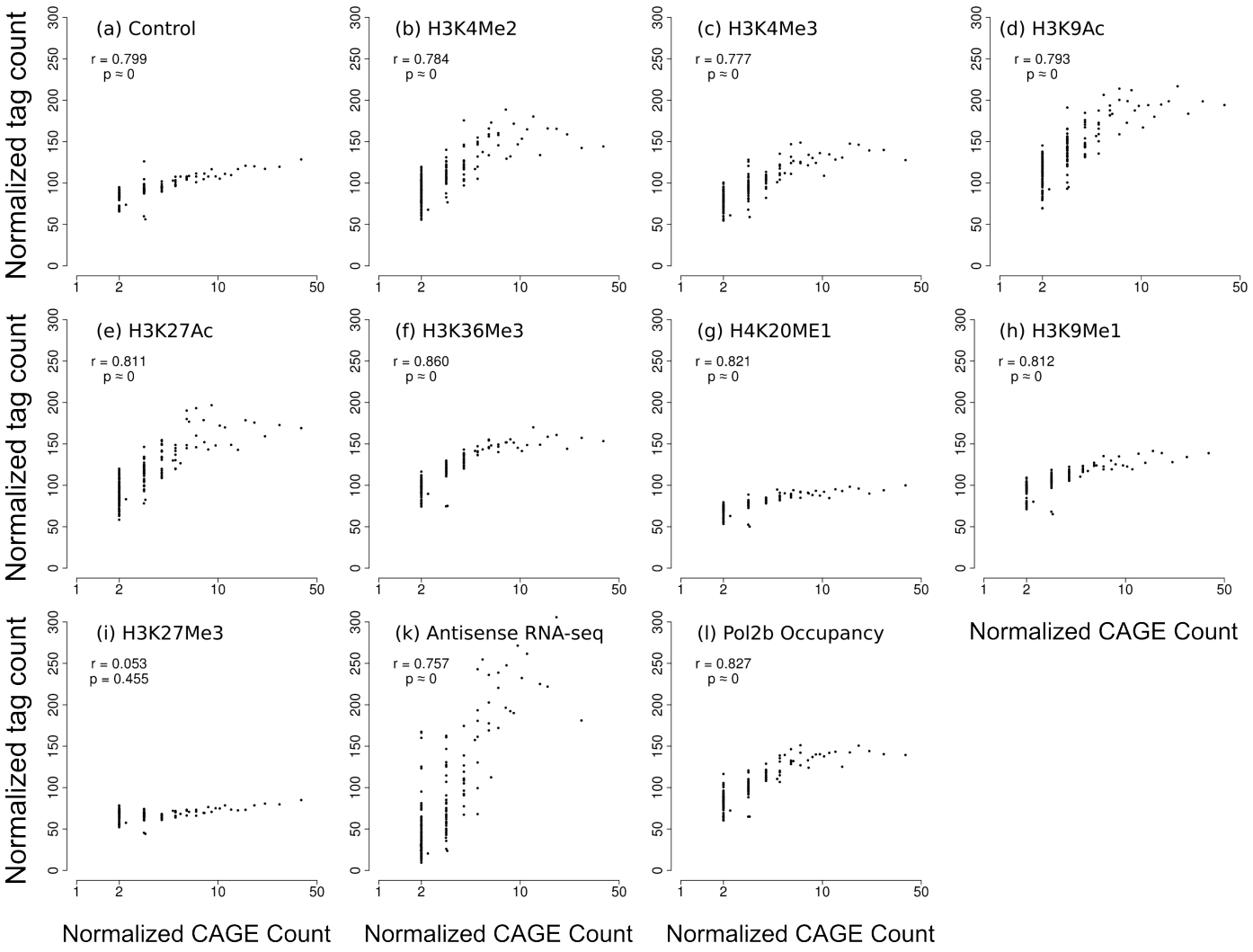

Supplementary Figure S26. Correlation between cis-NAT promoter activity and local chromatin environment in K562. Cis-NAT promoters in the K562 cell type were identified using CAGE data from total nucleolus isolates. Cis-NAT promoters were divided into 200 bins based on activity, as measured by CAGE tags counts, and the normalized average numbers of ChIP-seq reads for histone modifications and RNA Pol II binding +/- 5kb of the cis-NAT TSS were calculated. Spearman rank correlations were used to determine the relationship between cis- NAT promoter activity and local histone modifications or RNA Pol II occupancy.

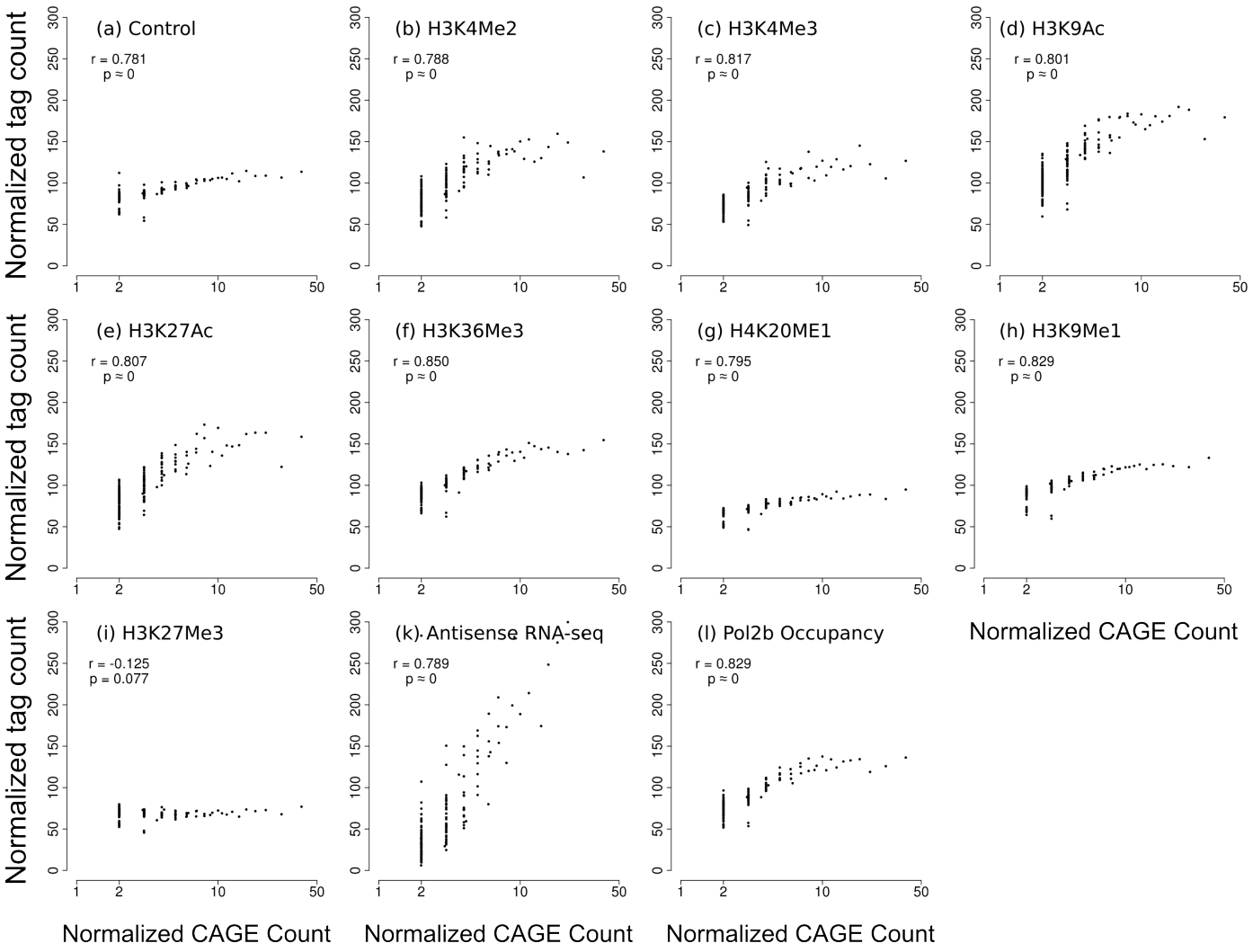

Supplementary Figure S27. Correlation between cis-NAT promoter activity and local chromatin environment in K562. Cis-NAT promoters in the K562 cell type were identified using CAGE data from total nucleoplasm isolates. Cis-NAT promoters were divided into 200 bins based on activity, as measured by CAGE tags counts, and the normalized average numbers of ChIP-seq reads for histone modifications and RNA Pol II binding +/- 5kb of the cis-NAT TSS were calculated. Spearman rank correlations were used to determine the relationship between cis-NAT promoter activity and local histone modifications or RNA Pol II occupancy.

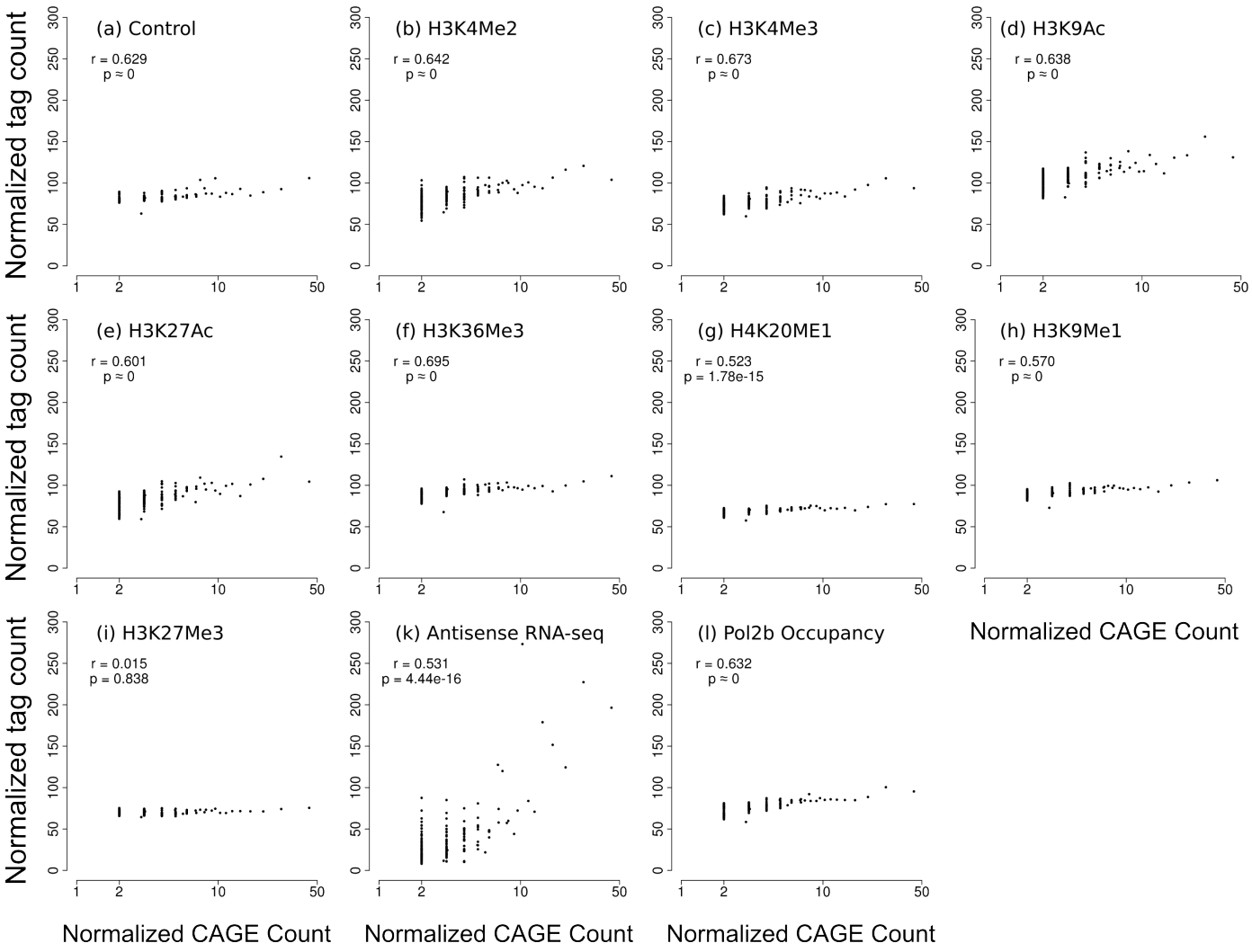

Supplementary Figure S28. Correlation between cis-NAT promoter activity and local chromatin environment in K562. Cis-NAT promoters in the K562 cell type were identified using CAGE data from non-polyadenylated nucleus isolates. Cis-NAT promoters were divided into 200 bins based on activity, as measured by CAGE tags counts, and the normalized average numbers of ChIP-seq reads for histone modifications and RNA Pol II binding +/- 5kb of the cis-NAT TSS were calculated. Spearman rank correlations were used to determine the relationship between cis-NAT promoter activity and local histone modifications or RNA Pol II occupancy.

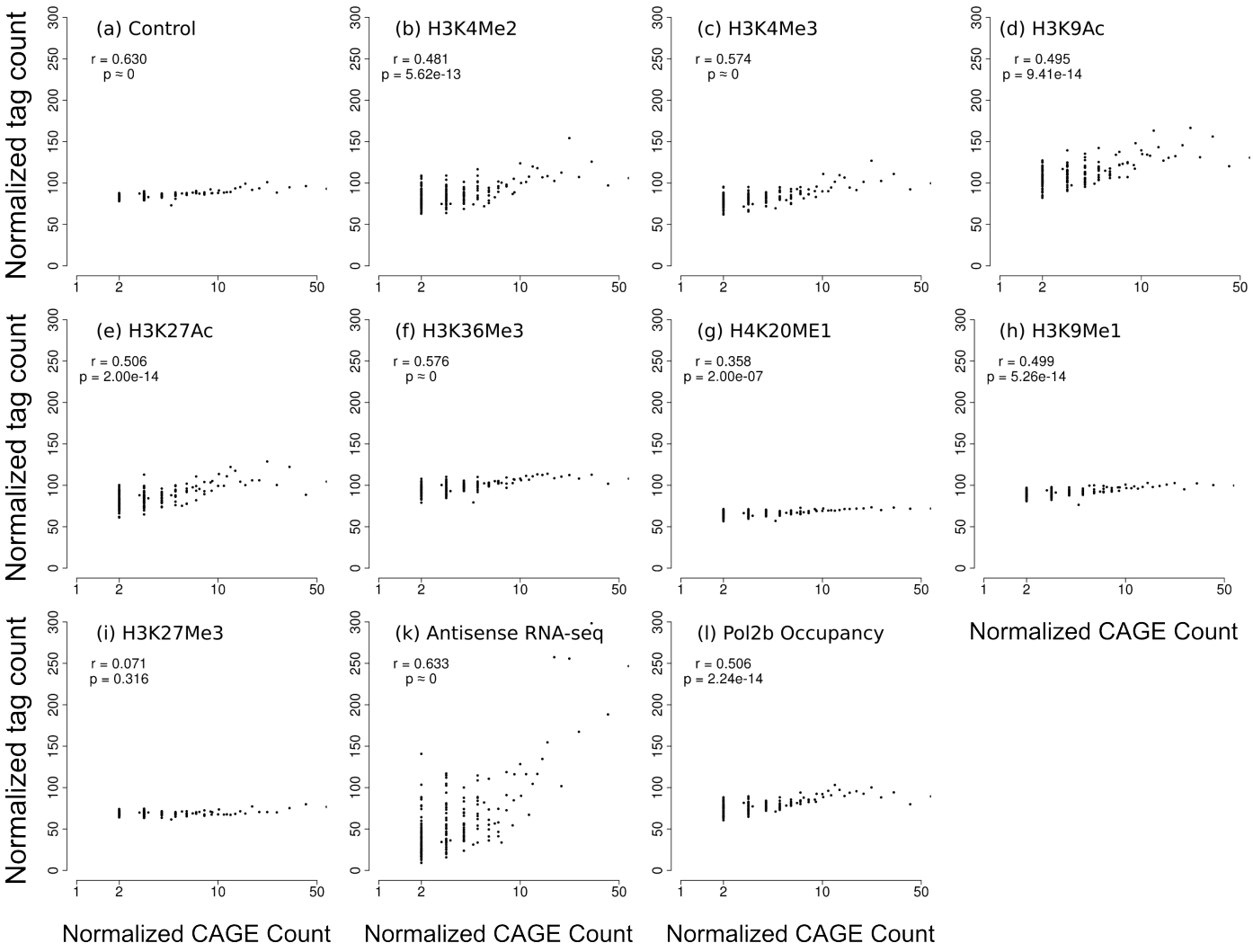

Supplementary Figure S29. Correlation between cis-NAT promoter activity and local chromatin environment in K562. Cis-NAT promoters in the K562 cell type were identified using CAGE data from polyadenylated nucleus isolates. Cis-NAT promoters were divided into 200 bins based on activity, as measured by CAGE tags counts, and the normalized average numbers of ChIP-seq reads for histone modifications and RNA Pol II binding +/- 5kb of the cis-NAT TSS were calculated. Spearman rank correlations were used to determine the relationship between cis-NAT promoter activity and local histone modifications or RNA Pol II occupancy.

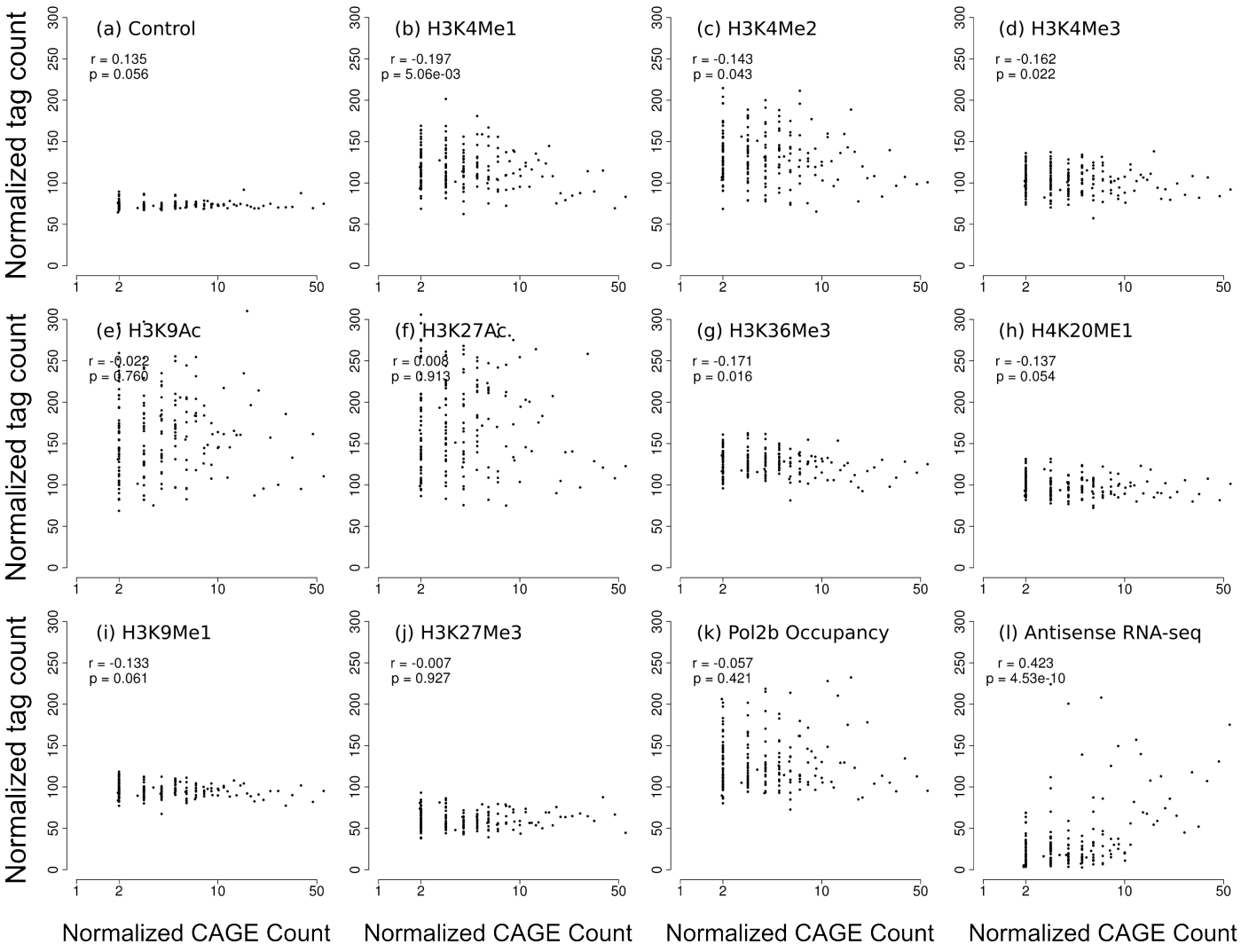

Supplementary Figure S30. Correlation between cis-NAT promoter activity and local chromatin environment in NHEK. Cis-NAT promoters in the NHEK cell type were identified using CAGE data from non-polyadenylated cytosol isolates. Cis-NAT promoters were divided into 200 bins based on activity, as measured by CAGE tags counts, and the normalized average numbers of ChIP-seq reads for histone modifications and RNA Pol II binding +/- 5kb of the cis-NAT TSS were calculated. Spearman rank correlations were used to determine the relationship between cis-NAT promoter activity and local histone modifications or RNA Pol II occupancy.

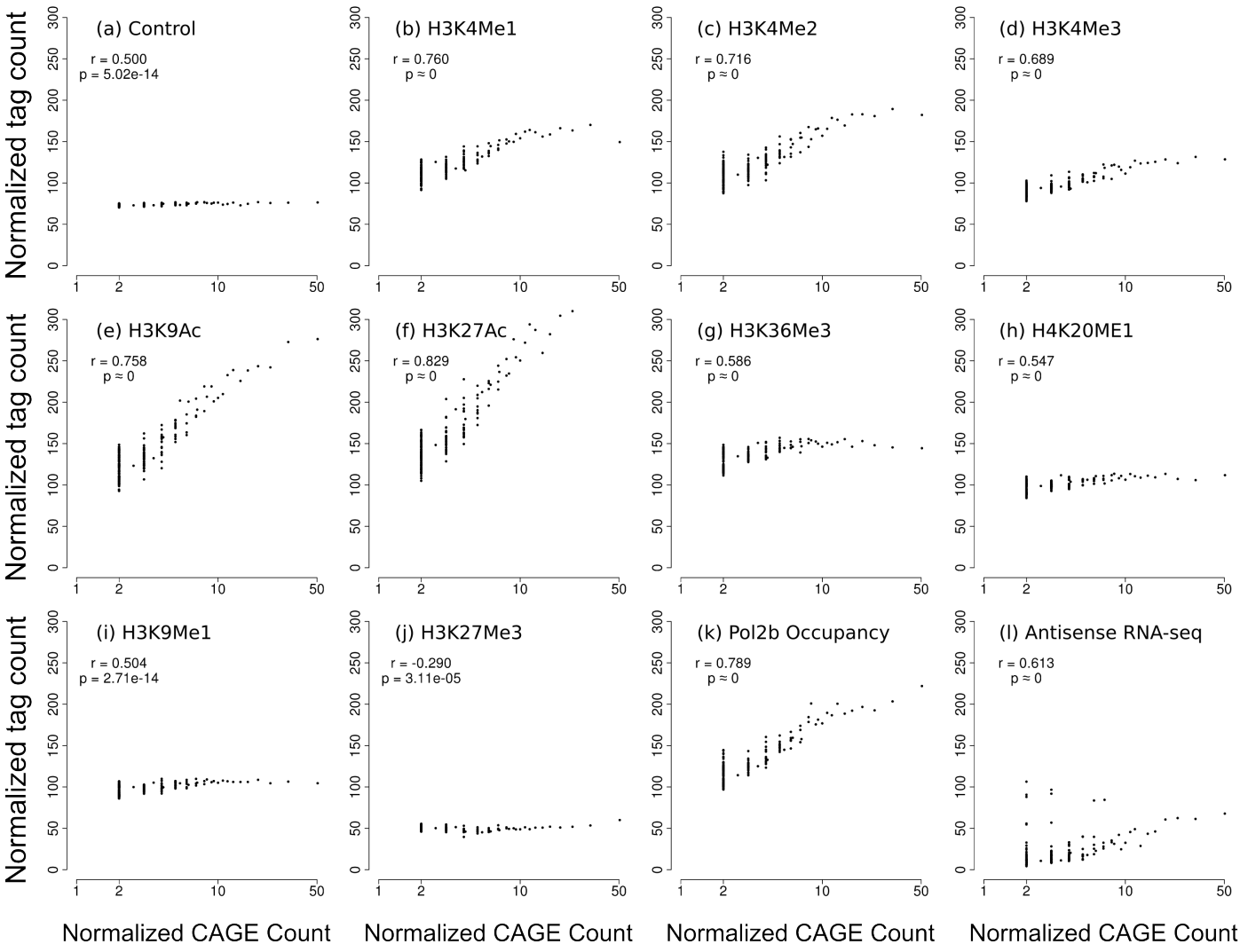

Supplementary Figure S31. Correlation between cis-NAT promoter activity and local chromatin environment in NHEK. Cis-NAT promoters in the NHEK cell type were identified using CAGE data from non-polyadenylated nucleus isolates. Cis-NAT promoters were divided into 200 bins based on activity, as measured by CAGE tags counts, and the normalized average numbers of ChIP-seq reads for histone modifications and RNA Pol II binding +/- 5kb of the cis-NAT TSS were calculated. Spearman rank correlations were used to determine the relationship between cis-NAT promoter activity and local histone modifications or RNA Pol II occupancy.